Pure appl. geophys. 152 (1998) 125–138
0033–4553/98/010125–14 $ 1.50 + 0.20/0

Pure and Applied Geophysics

P- and *S*-Wave Site Response of the Seismic Network RESNOM Determined from Earthquakes of Northern Baja California, Mexico

RAÚL R. CASTRO[1] and RESNOM WORKING GROUP[1]

Abstract—We determined the response to *P*- and *S*-wave incidence of the permanent stations of the seismic network of Baja California (RESNOM) using two independent methods. We selected 65 events with magnitudes between 2.2 and 4.8 and hypocentral distances ranging between 5 and 330 km. The site response of the ten stations analyzed was first estimated using average spectral ratios between the horizontal and the vertical components of motion (H/V ratios). As a second approach we performed a simultaneous inversion for source and site. In order to invert the spectral records to determine the site response, we made an independent estimate of the attenuation for two different source-station path regions. Then we corrected the spectral records for the attenuation effect before we made the inversion. Although the average H/V ratio of many sites is inside the error bars of the site response estimated with the spectral inversion, the spectral inversion tends to give higher values. For the *S* wave some sites show similar frequency of predominant peak when comparing the responses obtained with both methods. In contrast, for the *P* waves the H/V ratios disagree with the results of the inversion. In general, the site response of the stations is strongly frequency dependent for both *P* and *S* waves. We also found that the natural frequency of resonance of the sites is near 0.5 Hz for *P* and near 0.8 Hz for the *S* waves.

Key words: Site response, earthquakes of Baja California.

Introduction

Recent studies of site amplification (SILVA and DARRAGH, 1995; STEIDL *et al.*, 1996; BOORE and JOYNER, 1997) emphasize the importance of evaluating the seismic response of rock sites because of the practical implications of this on building codes and seismic design. CASTRO *et al.* (1990), for instance, found amplification factors on rock sites as high as 5.0 for stations of the Guerrero Accelerograph Array, and BOORE and JOYNER (1997) found factors as high as 3.5 at high frequencies. The seismic network of Baja California (RESNOM) also offers a good opportunity to study the site amplification of rock sites, since most of the

[1] División Ciencias de le Tierra, CICESE, Apartado Postal 2732, Ensenada, Baja California, México. Fax: (011-5261) 75 05 59, e-mail: raul@cicese.mx

stations of this network are located on rock sites. The signals of the three-component stations are digitized at 40 samples per second and sent by telemetry to the central base in CICESE, Ensenada. In order to make the links between the stations and the central base, the stations were located on hills or high elevation points. Thus, the data from this network can also be used to study the effects of the topography on the ground motion.

To evaluate the site effects we used two techniques, first we calculate an average spectral ratio between the horizontal and the vertical component of motion (H/V ratios) for each station analyzed. Then, as a second approach, we determined the site function of the stations using a spectral inversion.

Data

We selected three-component records from 65 earthquakes recorded by at least six stations with clear *P*- and *S*-wave arrivals. Figure 1 shows the location of the epicenters and the stations used in the analysis, and Table 1 lists the coordinates and elevations of the stations. The earthquakes selected have magnitudes between 2.2 and 4.8. All the focal depths are less than 20 km and the hypocentral distances vary between 5 and 330 km.

The records were base-line corrected by subtracting the mean to remove long-period biases. Then, we calculated the Fourier transform of two time windows for each component of motion, one containing *P* waves and another the *S* waves. The duration of the windows varied between 1.5 and 2.5 for the *P* waves and between 2.5 and 4.0 s for the *S* waves. The beginning and the end of the windows were tapered with a 10% cosine taper and the spectral amplitudes were smoothed with a one-third octave band moving window and corrected for the effect of the instrument response. Since the signals recorded by the network are filtered with a five-pole Butterworth antialiasing filter with a 15 Hz corner frequency (Hinojosa *et al.*, 1984; Vidal, 1987), we selected for the analysis only 18 amplitudes between 0.3 and 15 Hz.

Method

H/V Ratios

In order to eliminate the effects of source and attenuation along the source-station path, we calculated the spectral ratio between the horizontal and the vertical component of motion for each event. This technique is based on the assumption that the vertical component of motion shares the same attenuation and source effects as the horizontal component but is not influenced by site effects. The idea was first proposed by LANGSTON (1977) to study the crustal structure using long-period teleseismic signals. This technique has been used to study site amplification effects from regional earhtquakes by LERMO and CHAVEZ-GARCÍA (1993); FIELD and JACOB (1995); CASTRO *et al.* (1996); among others. H/V ratios have also been successfully applied to determine sediment-induced amplification using microtremors (NOGOSHI and IGARASHI, 1970; NAKAMURA, 1989).

Although the H/V ratios are usually applied to estimate the overall frequency dependence of the *S*-wave site response, in this paper we also tested the validity of

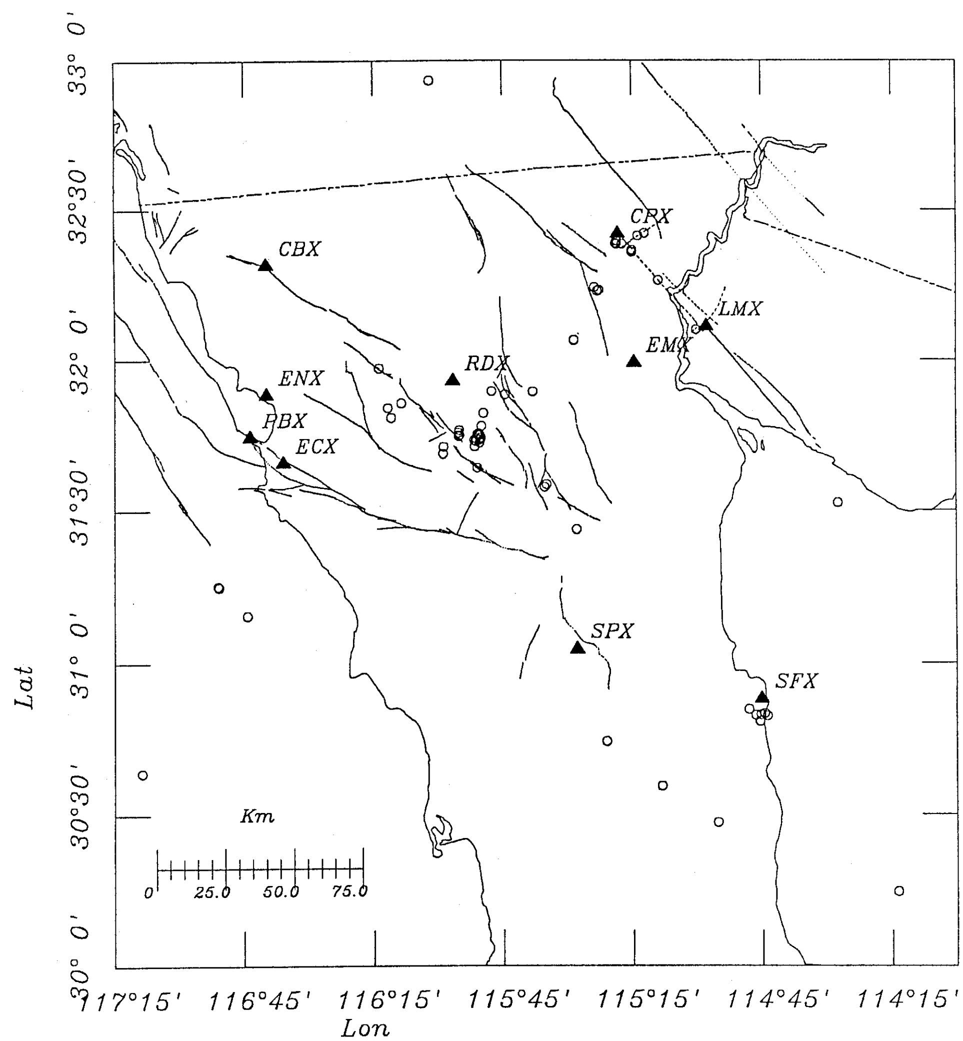

Figure 1
Distribution of stations (triangles) and epicenters (circles) used.

Table 1

Coordinates of the stations of the seismic network RESNOM

Station	Code	Lat. N	Lon. W	Elev. m	Site Geology
Cerro Bola	CBX	32.3132	116.6637	1215	Rhyolite
Cerro Prieto	CPX	32.4178	115.304	180	Basalt
Esteban Cantú	ECX	31.6570	116.5978	1040	Rhyolite
El Mayor	EMX	31.9882	115.2417	10	Granite
Ensenada	ENX	31.8835	116.6627	230	Rhyolite
La Mesa	LMX	32.1088	114.9627	25	Sand
Punta Banda	PBX	31.7420	116.7255	330	Volcanic rock
Rancho Dawing	RDX	31.9282	115.9422	708	Granodiorite
San Felipe	SFX	30.8812	114.7522	55	Granite
San Pedro Mártir	SPX	31.0452	115.4637	2835	Granodiorite

the method for P waves. For each station we averaged the H/V ratios over all the events recorded and then we calculated the average of the two components. Figure 2 shows the average H/V ratio calculated using the P-wave spectral records (black dots) and the S-wave spectra (open circles). The light and dashed lines signify the standard deviation calculated for the P- and S-wave ratios, respectively. A common feature of the site response of the stations is that the amplification tends to be higher for the P waves (solid lines) and that for most of the stations the amplification level is below two. In spite of being on hard rock, the station San Pedro Martir (SPX) shows higher amplification levels than the other stations. It is also interesting to note in Table 1 that SPX is located on a high altitude site (2835 m).

Spectral Inversion

Another approach to estimate the site response of the RESNOM stations is to consider all the factors affecting the observed spectral amplitudes in a simultaneous inversion. Thus, for a given frequency the ground motion spectra can be represented as:

$$U_{ij}(f,r) = S_i(f) \cdot Z_j(f) \cdot A(f,r) \tag{1}$$

where $S_i(f)$ accounts for source-related effects of earthquake i, $Z_j(f)$ represents the site effects of station j and $A(f,r)$ is the attenuation function which accounts for the amplitude decay due to geometrical spreading and anelastic attenuation (Q). In equation (1) it is implicitly assumed that all the source-station paths share the same attenuation characteristics. However, based on previous attenuation studies in the region (Singh *et al.*, 1982; Castro, 1983; Rebollar *et al.*, 1985; among others), we expect regional variations of $A(f,r)$. In particular, the attenuation along source-station paths inside the Peninsular Ranges, in the western part of the region, is different than the attenuation along paths inside the Mexicali-Imperial Valley. Thus, instead of solving equation (1) simultaneously for source, site and attenuation, we will determine $A(f, r)$ separately for the two regions and then we will solve equation (1) for source and site terms after we correct the spectral records for the appropriate attenuation effect.

In order to make the regional estimates of $A(f, r)$, the data set was separated accordingly in two groups: one group was formed with records from stations located in the Valley of Mexicali (CPX, LMX, EMX, SFX) that recorded events

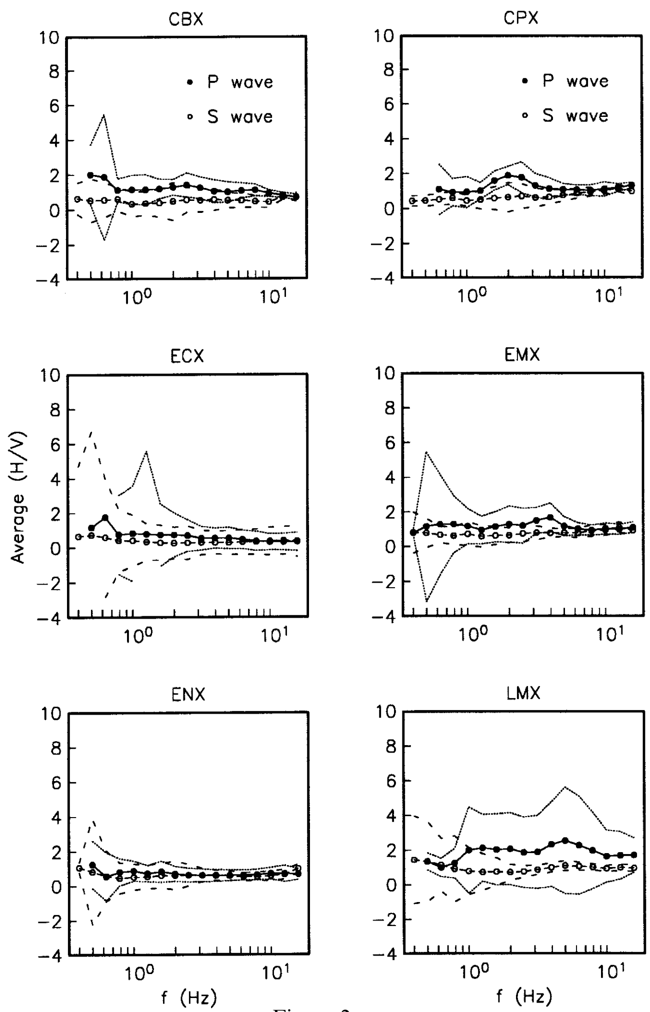

Figure 2

Average H/V ratios calculated using *P*-wave (black dots) and *S*-wave (open circles) spectral records. The light lines and the dashed lines correspond to the mean ±1 standard deviation computed for the *P*- and the *S*-wave spectra, respectively.

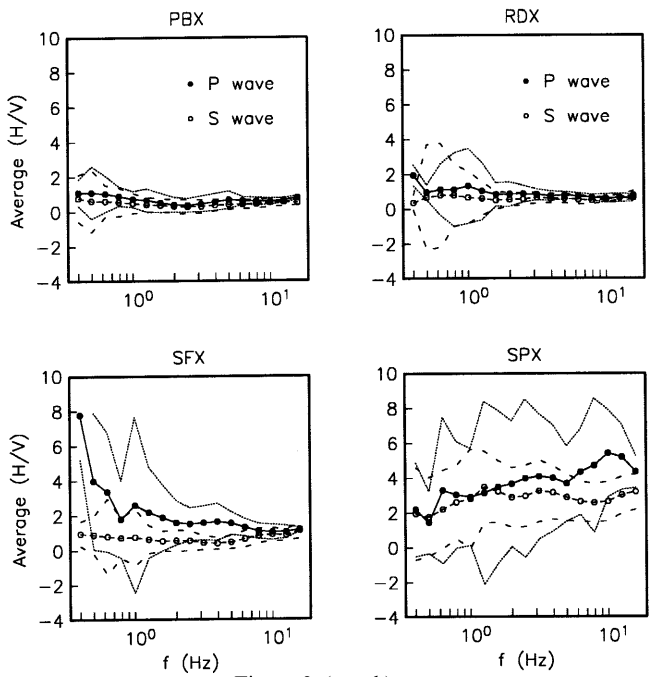

Figure 2 *(contd.)*

located to the east of Sierra Juarez (east of RDX) and Sierra San Pedro Martir (east of SPX), and a second group with records from events and stations located in the Peninsular Ranges (stations in the central and western side of the Peninsula). We obtained attenuation functions (one for each frequency considered) for both P and S waves by fitting the observed amplitude decay with smooth functions of distance using a nonparametric model (e.g., ANDERSON and QUAAS, 1988; CASTRO *et al.*, 1990; ANDERSON, 1991). In this model the spectral amplitudes depend only on the size of the i-th earthquake, represented by a scalar factor $S_i(f)$, and the attenuation function $A(f, r)$:

$$U_i(f, r) = S_i(f) \cdot A(f, r). \tag{2}$$

The attenuation function in equation (2) contains the effects of Q and geometrical spreading and is not limited to a particular functional form. However, it is assumed that $A(f, r)$ is a smooth function that decreases with distance. The inversion scheme used to retrieve $A(f, r)$ using equation (2) is described in detail by CASTRO *et al.* (1990, 1996) and ANDERSON (1991). In this approach the site response becomes the residual which results from solving equation (2), e.g.,

$$Z(f) = S_i(f) \cdot A(f, r)/U_i(f, r). \tag{3}$$

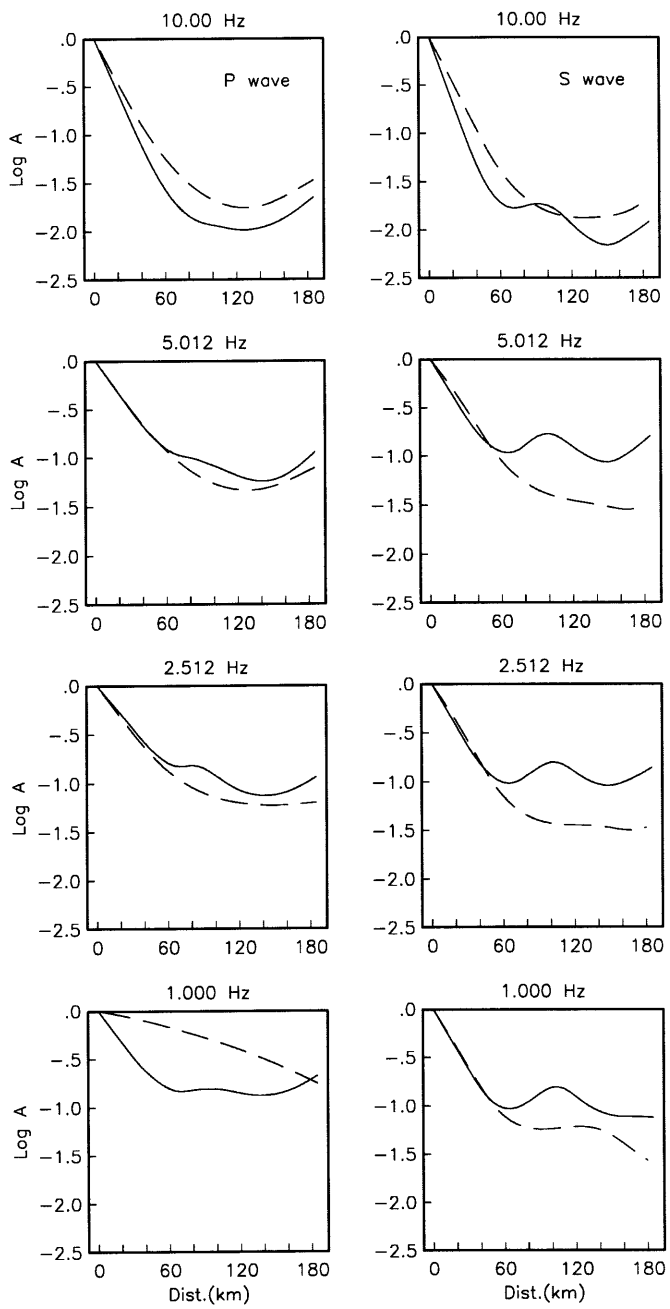

Figure 3
Attenuation functions obtained for source-station paths inside the Peninsular Ranges (solid lines) and for paths inside the Mexicali Valley (dashed lines). The frames on the left correspond to the functions obtained for the *P* waves and the frames on the right to the *S* waves.

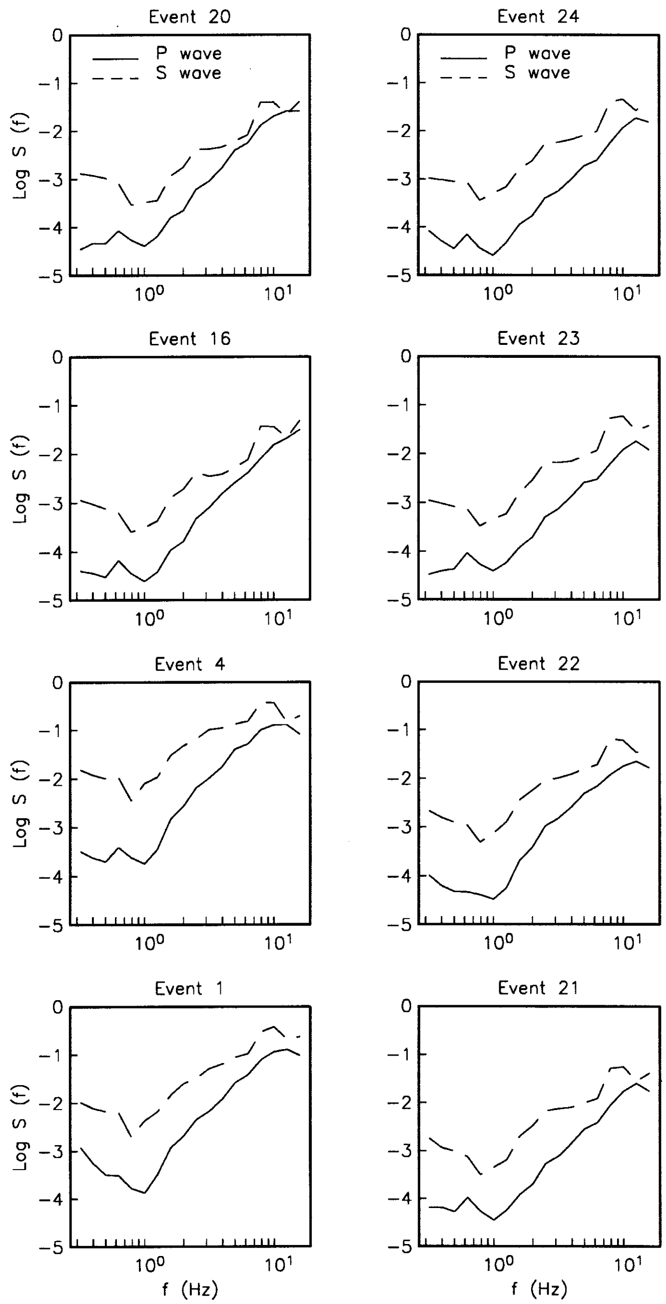

Figure 4
Sample of acceleration source functions obtained using *P* waves (solid lines) and *S* waves (dashed lines).

Once we determine $A(f, r)$ at each frequency analyzed, we can correct the spectral records for the attenuation effect, so that equation (1) can be written as

$$d_{ij} = s_i + z_j \tag{4}$$

where $d_{ij} = \mathrm{Log}(U_{ij}(f, r)/A(f, r))$, $s_i = \mathrm{Log}(S_i(f))$ and $z_i = \mathrm{Log}(Z_j(f))$. Equation (4) represents an overdetermined system of equations that can be solved for s_i and z_j. Due to the linear dependence existing between the site and the source terms, there is one undertermined degree of freedom in equation (4). To eliminate this linear dependence, we solved equation (4) constraining the logarithm of the site response factor at EMX to zero, irrespective of frequency. We selected EMX as the reference station because it is located on granite, it has a good operating history and we do not expect topographic effects since it is also located at low altitude (10 m). Note in Figure 2 that EMX has an average H/V ratio close to 1 for both *P* and *S* waves, suggesting small amplifications for this site.

Results

We determine attenuation functions for 18 frequencies using the nonparametric model (equation 2) for both *P* and *S* waves. Figure 3 displays the attenuation functions obtained for 1.0, 2.5, 5.0 and 10.0 Hz. The frames on the left show the functions obtained for the *P* waves and the frames on the right for the *S* waves. In general, $A(f, r)$ decays faster with distance for the *P* waves, indicating greater attenuation for *P* relative to *S* waves. In Figure 3 we also compare the attenuation between the two regions. At high frequencies ($f = 10.0$ Hz) the attenuation curves obtained for the Mexicali Valley (dashed lines) indicate lower attenuation at short distances ($r < 60$) for both *P* and *S* waves and approximately the same rate of amplitude decay for lower frequencies, when we compare with the curves for the Peninsular Ranges. This consistent with previous attenuation studies made in these regions. For instance, REBOLLAR *et al.* (1985) found in the Peninsular Ranges that at short distances (~ 16 km) $Q_s = 65$ and $Q_p = 57$ while at longer distances (~ 83 km) $Q_s = 700$ and $Q_p = 397$, for a frequency band between 3 and 24 Hz. On the other hand, SINGH *et al.* (1982) found that $Q_s = 20\ f$ in the Imperial-Mexicali Valley. This implies that at 10 Hz the attenuation must be stronger in the Peninsular Ranges at short distances, consistent with the curves shown in Figure 3. For longer distances and lower frequencies ($1.0 < f < 2.2$ Hz), CASTRO (1983) found that $Q_s = 350$ along the Peninsular Ranges and $Q_s = 170$ in the Imperial-Mexicali Valley. This result is also consistent with the *S*-wave attenuation functions shown in Figure 3 for $f < 5$ Hz.

It is also interesting to note that for the *S* waves the attenuation functions obtained for paths along the Peninsular Ranges show a maximum at about 100 km. For the *P* waves, however, the 100 km peak is less prominent, in particular at 1 Hz.

This increase of $A(f, r)$ may be due to reflections from the base of the crust as observed in other regions (SOMERVILLE and YOSHIMURA, 1990) or other wave propagation mechanisms that we cannot determine with the model adopted.

As mentioned, in order to evaluate the site effects we used these attenuation functions to correct the spectral records according to their regional source-station paths so that, after the attenuation correction, we solved the source and site terms using equation (4) and constraining the logarithm of the site response at EMX to zero. Figure 4 illustrates a sample of acceleration source functions obtained from

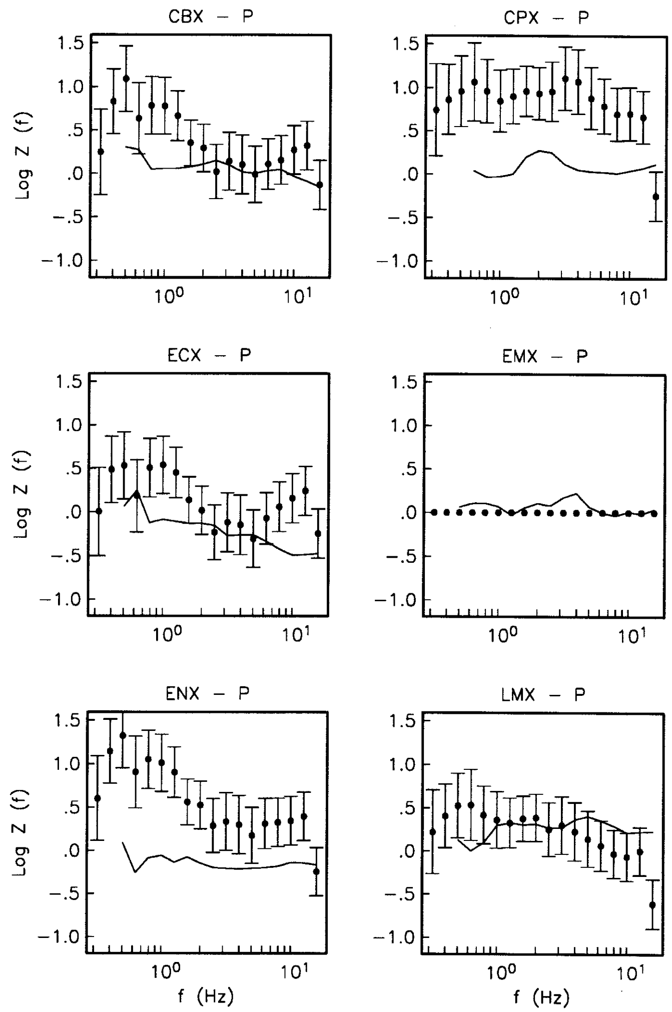

Figure 5
P-wave site response. Solid lines are the average H/V raitos obtained and the dots with error bars are the estimates obtained using the spectral inversion.

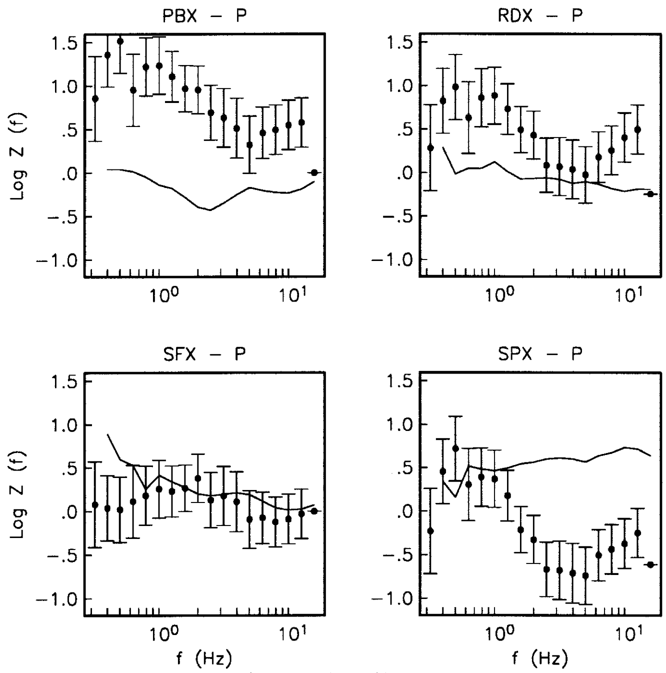

Figure 5 *(contd.)*

the *P* (solid lines) and the *S* waves (dashed lines). Since the events analyzed have small magnitudes ($2.2 < M < 4.8$) and most of them have magnitudes less than 3.9, their corner frequencies are generally beyond the frequency band analyzed. However, it is interesting to note that, at low frequencies ($f < 10$ Hz), the amplitudes of the *S*-wave source functions are, as expected, above those obtained for the *P* waves.

The seismic response of the sites resulting from the spectral inversion is shown in Figure 5 for the *P* waves and in Figure 6 for the *S* waves. For comparison we also plotted in these figures the site functions obtained using H/V ratios. For *P* waves the average H/V ratio (solid line) gives functions that are different than those obtained from the inversion (black dots). This result suggests that for the *P* waves the H/V ratios do not give reliable estimates of the site response. However, for the *S* waves (Fig. 6) the shapes of the functions obtained with both techniques are similar, although for all the sites, except SPX, the amplification level predicted by the H/V ratio (dashed lines) is below that obtained with the inversion (open circles). Other studies of site effects (LACHET and BARD, 1994; FIELD and JACOB, 1995; BONILLA *et al.*, 1997) have found that the resonance frequency obtained from H/V ratios is similar to that obtained using *S*-wave inversions. However, they found that the amplification is different from that estimated with spectral inversions.

The discrepancy of the amplification levels shown in Figure 6 is probably due to the different site reference used. While in the inversion we used a common reference

(EMX) for all the sites, for the H/V ratios each site has a specific site reference which depends on the particular characteristics of the basement below the site.

Conclusions

The discrepancy between the *P*-wave site response obtained using H/V ratios and that obtained from the spectral inversion suggests that the former technique is not reliable for evalutaions of *P*-wave response. We also observed that the H/V

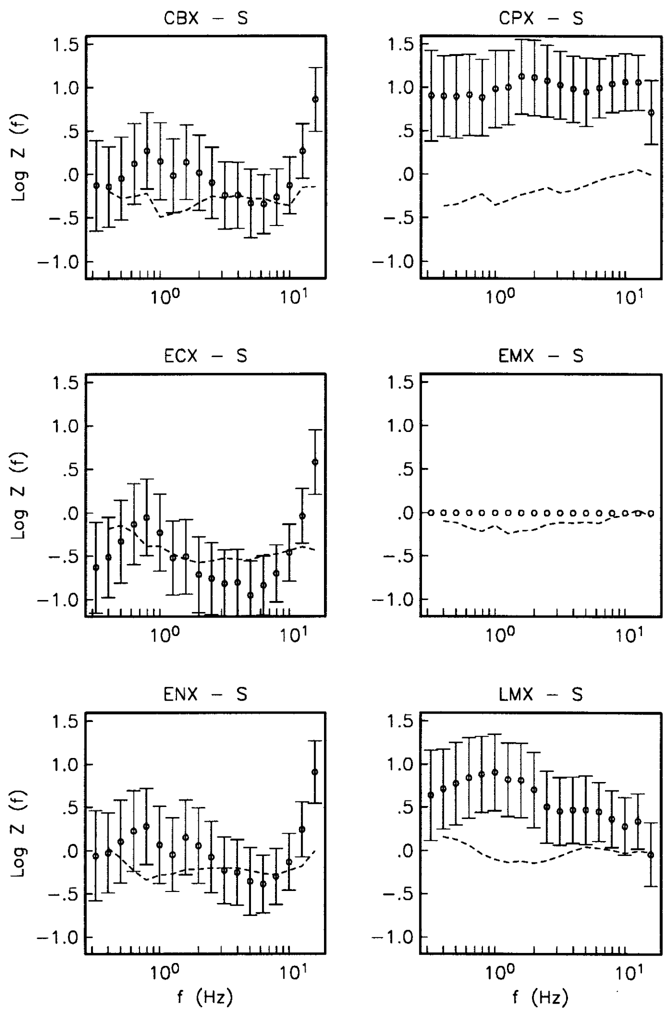

Figure 6
S-wave site response. Dashed lines correspond to the average H/V ratios and the circles with error bars the estimates obtained using the spectral inversion.

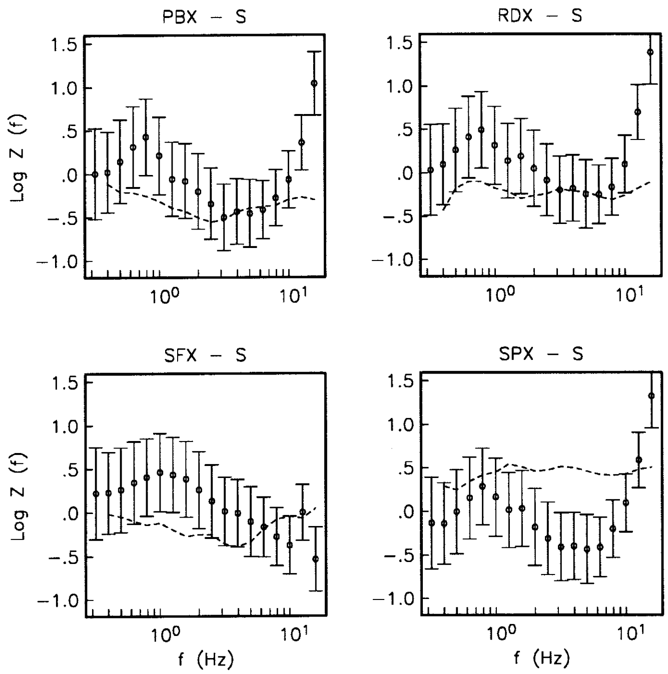

Figure 6 *(contd.)*

ratios give higher amplification factors for both *P* and *S* waves for station SPX, which is located at a high elevation mountain in Sierra San Pedro Martir. This observation suggests that the topography may have a stronger effect on the site response when this is evaluated using H/V ratios than when is obtained using the spectral inversion. The results obtained from the spectral inversion manifest a strong dependence of the site response with frequency for both *P* and *S* waves. For the *P* waves, most sites have a natural frequency of resonance near 0.5 Hz, and a maximum amplification, relative to EMX, that varies from a factor of 33 at CBX to a factor of 2.4 at SFX. In contrast, for the *S* waves the resonant frequency of most sites is at 0.8 Hz and the maximum amplification is a factor of 13 at CPX. We also observed that the station ECX shows deamplification between 0.3 and 13 Hz and SPX between 1.6 and 15 Hz.

Acknowledgments

This investigation was partially supported by the Mexican National Council of Science and Technology (CONACYT). Guadalupe Rodríguez and Urivan Flores participated in preprocessing the data. We are thankful to Dr. Dave Boore for providing helpful comments that improved the original manuscript.

References

Anderson, J. G., and Quaas, R. (1988), *The Mexico Earthquake of September 19, 1985: Effect of Magnitude on the Character of Strong Ground Motion: An Example from the Guerrero, Mexico Strong Motion Network*, Earthquake Spectra *4*, 635–646.

Anderson, J. G. (1991), *A Preliminary Descriptive Model for the Distance Dependence of the Spectral Decay Parameter in Southern California*, Bull. Seismol. Soc. Am. *81*, 2186–2193.

Bonilla, L. F., Steidl, J. H., Lindley, G. T., Tumarkin, A. G., and Archuleta, R. J. (1997), *Site Amplification in the San Fernando Valley, California: Variability of Site-effect Estimation Using the S Wave, Coda, and H/V Methods*, Bull. Seismol. Soc. Am. *87*, 710–730.

Boore, D. M., and Joyner, W. B. (1997), *Site Amplifications for Generic Rock Sites*, Bull. Seismol. Soc. Am. *87*, 327–341.

Castro, R. R. (1983), *Source Parameters and Propagation-path Effects for Earthquakes in the Baja California Norte and Imperial Valley Regions*, M.S. Thesis, University of California, San Diego, La Jolla, California.

Castro, R. R., Anderson, J. G., and Singh, S. K. (1990), *Site Response, Attenuation and Source Spectra of S Waves along the Guerrero, Mexico, Subduction Zone*, Bull. Seismol. Soc. Am. *80*, 1418–1503.

Castro, R. R., Pacor, F., Sala, A., and Petrungaro, C. (1996), *S-wave Attenuation and Site Effects in the Region of Friuli, Italy*, J. Geophys. Res. *101*, 22,355–22,369.

Field, E. H., and Jacob, K. H. (1995), *A Comparison and Test of Various Site-response Estimation Techniques Including Three that are not Reference-site Dependent*, Bull. Seismol. Soc. Am. *85*, 1127–1143.

Hinojosa, A., Duarte, C., and Inzunza, L. (1984), *Sistema de adquisición y procesamiento RESNOR*, Technical Report CICESE, 84–01.

Lachet, C., and Bard, P. Y. (1994), *Numerical and Theoretical Investigations on the Possibilities and Limitations of Nakamura's Technique*, J. Phys. Earth *42*, 377–397.

Langston, C. A. (1977), *Corvallis, Oregon, Crustal and Upper Mantle Receiver Structure from Teleseismic P and S Waves*, Bull. Seismol. Soc. Am. *67*, 713–724.

Lermo, J., and Chavez-Garcia, F. J. (1993), *Site Effect Evaluation Using Spectral Ratios with only one Station*, Bull. Seismol. Soc. Am. *83*, 1574–1594.

Nakamura, Y. (1989), *A Method for Dynamic Characteristics Estimation of Subsurface Using Microtremor on the Ground Surface*, Q. R. Railway Tech. Res. Inst. Rep. *30*, 25–33.

Nogoshi, M., and Igarashi, T. (1970), *On the Propagation Characteristics of Microtremor*, J. Seismol. Soc. Jpn. *23*, 264–280.

Rebollar, C. J., Traslosheros, C., and Alvarez, R. (1985), *Estimates of Seismic Wave Attenuation in Northern Baja, California*, Bull. Seismol. Soc. Am. *75*, 1371–1382.

Silva, W. J., and Darragh, R. B. (1995), *Engineering Characterization of Strong Ground Motion Recorded at Rock Sites*, Electric Power Research Institute, Palo Alto, California, Report No. TR-102262.

Singh, S. K., Aspel, R. J., Fried, J., and Brune, J. N. (1982), *Spectral Attenuation of SH Waves along the Imperial Fault*, Bull. Seismol. Soc. Am. *72*, 2003–2016.

Somerville, P., and Yoshimura, J. (1990), *The Influence of Critical Moho Reflections on Strong Ground Motions Recorded in San Francisco and Oakland during the 1989 Loma Prieta Earthquake*, Geophys. Res. Lett. *17*, 1203–1206.

Steidl, J. H., Tumarkin, A. G., and Archuleta, R. J. (1996), *What is a Reference Site?*, Bull. Seismol. Soc. Am. *86*, 1733–1748.

Vidal, A. (1987), *Magnitud local y parámetros de fuente para sismos de la zona de fallas San Miguel-Vallecitos, Baja California*, M.S. Thesis, Centro de Investigación Científica y de Educación Superior de Ensenada, Ensenada Baja California, México.

(Received June 23, 1997, accepted November 12, 1997)